Interface Study by Dual Beam FIB-TEM in a pressureless infiltrated Al(Mg) / Al_2O_3 Interpenetrating Composite

H. Chang*, R. L. Higginson & J. G. P. Binner

IPTME, Loughborough University, Loughborough, LE11 3TU, UK

*Corresponding author. E-mail: H.chang@lboro.ac.uk

Tel: + 44 (0) 1509 263171 4361; Fax: +44 (0) 1509 223949

Abstract

This paper considers the microstructures of an Al(Mg)/Al_2O_3 interpenetrating composite produced by a pressureless infiltration technique. It is well known that the governing principle in pressureless infiltration in Al/Al_2O_3 system is the wettability between the molten metal and the ceramic phase; however, the infiltration mechanism is still not well understood. The objective of this research was to observe the metal / ceramic interface to understand the infiltration mechanism better. The composite was produced using an Al-8wt.% Mg alloy and 15% dense alumina foams at 915°C in a flowing N_2 atmosphere. After infiltration, the composite was characterized by a series of techniques. Thin film samples, specifically produced across the Al(Mg)-Al_2O_3 interface, were prepared using a Dual Beam Focused Ion Beam (FIB) and subsequently observed using Transmission Electron Microscopy (TEM). XRD scan analysis shows that Mg_3N_2 formed in the foam at the molten alloy-ceramic infiltration front whilst TEM analysis revealed that fine AlN grains formed at the metal / ceramic interface and $MgAl_2O_4$ and $MgSi_2$ grains formed at specific points. It is concluded that it is the reactions

between the Al, Mg and N_2 atmosphere that improve the wettability between molten Al and Al_2O_3 and induce spontaneous infiltration.

Introduction

Aluminium alloys reinforced with ceramic particles or fibres are desired composites in high performance applications due to their superior properties; light weight combined with high modulus, strength, hardness and wear resistance; good thermal conductivity and reduced coefficient of thermal expansion. Compared with traditional particulate or fibre reinforced composites, 3-3 interpenetrating composites with both matrix and reinforcement co-continuous throughout the microstructure are more attractive in providing superior application-tailored multifunctional and novel properties (Clarke, 1992). The pressureless infiltration of molten metals into ceramic foams (Binner *et al.,* in press) is potentially superior to more traditional methods such as squeeze casting, having the advantages of there being no requirement for high pressure and hence offering potentially low cost and near net shape production. However, due to the poor wettability between molten aluminium and ceramics, pressureless infiltration requires the presence of both Mg and a nitrogenous infiltration atmosphere (Aghjanian *et al.,* 1991). Although it is widely accepted that Mg is a strong surfactant and it improves the wettability of molten Al with Al_2O_3 (Zhong *et al.,* 1989), the infiltration mechanism is still not completely understood.

Rao and Jayaram (Rao & Jayaram, 2001) investigated the pressureless infiltration of Al-Mg-based alloys into alumina preforms and concluded that the role of Mg was

two fold, namely, in initiating, and then continuing, infiltration. Initiation was caused by the reaction(s) of Mg with the surface Al_2O_3 to form a non-protective oxide layer, which eroded the passivating Al_2O_3 layer and brought about the contact between the molten metal and the ceramic preform. The continuation of the infiltration was caused by the Mg gathering oxygen, therefore keeping the front free of passivating alumina, whilst termination was due to localised Mg depletion at the infiltration front. The Mg loss might have resulted from Mg evaporation or the formation of MgO and $MgAl_2O_4$. However, from a study of the role of Mg and N_2 during the spontaneous infiltration of aluminium eutectic alloys into partially nitrided AA6061 aluminium powder preforms, Sercombe and Schaffer (Sercombe & Schaffer, 2004) concluded that the formation of AlN was critical for the infiltration; Mg was beneficial, but not sufficient. They concluded that AlN improved the wettability and facilitated spontaneous infiltration; whereas Mg was helpful in scavenging the oxygen and, as a result, creating a microclimate with extremely low oxygen partial pressure that facilitated the formation of the AlN. Saravanan *et al.* (Saravanan *et al.,* 2001) studied the effect of N_2 on Al surface tension and reported that N_2 greatly reduced it well below the values found in an Ar atmosphere at temperatures higher than 850°C as a result of the formation of AlN.

Based on the fact that both Mg and N_2 are needed for the pressureless infiltration, another assumption is that the spontaneous infiltration is dependent on the reaction between Mg and N_2 to form Mg_3N_2 (Lee *et al.,* 1998):

$$3Mg + N_2 \rightarrow Mg_3N_2 \quad (1)$$

This then reacts with Al to form AlN:

$$Mg_3N_2 + 2Al \rightarrow 2AlN + 3Mg \quad (2)$$

It is believed that reaction (2) is important in improving wetting and aids infiltration (Schiroky *et al.,* 1997), the overall reaction being:

$$Al + N_2 \rightarrow AlN \quad (3)$$

Mg is retained in the cycle and reintroduced to the melt, which acts as a catalyst (Hou *et al.,* 1995).

This research considers the microstructures formed in Al(Mg)/Al_2O_3 interpenetrating composites produced using the pressureless infiltration technique. The fine-scale microstructure at the Al-Al_2O_3 interface was observed using TEM. Schematics of the infiltration, the interfacial development processes and the reactions that might assist the infiltration are discussed.

Experimental

Alumina foams, with a density of 15 wt.% and an average cell diameter of 60 μm, were manufactured by Dytech Corp. Ltd, UK, using a gel-casting technique (Sepulveda & Binner, 1999). The metal infiltrant, an Al-8Mg alloy, was prepared from commercially pure Al and an Mg-Al master alloy AZ81 using an approach described elsewhere (Binner *et al.,* in press).

To fabricate the composites, discs of alumina foams measuring 50 × 20 × 9 mm were placed on top of an Al-8Mg alloy disc of the same size, the foam/alloy couples being held in alumina boats[1]. The arrangement was then heated at 20°C min^{-1} in a tube furnace in an argon atmosphere; to avoid temperature overshoot,

[1] Note: It made no difference whether the ceramic foams were placed on top of the alloy discs or vice versa.

the heating rate was reduced to 5°C min^{-1} from 850°C-915°C. Once the temperature reached 915°C, the argon atmosphere was switched to flowing pure nitrogen. A holding time of 20 mins at 915°C was used in order to obtain complete infiltration. To minimise metal shrinkage porosity, the composites were cooled at 15 - 20°C min^{-1} in flowing argon to 680°C, followed by furnace cooling in static argon at 5 - 10°C min^{-1} to room temperature. Partially infiltrated samples were obtained by holding the metal-ceramic couple at 915°C in N_2 for 10 mins followed by the same cooling process in N_2.

Following production, the composites were cut longitudely then ground and polished metallographically using diamond paste with a final polishing using 0.02 μm colloidal silica. The density of the composites was measured based on the Archimedean principle using a hydrostatic balance with a resolution of 0.1 g cm^{-3}. At least 3 measurements were performed on each sample. The microstructures of the alumina foams and the composites were examined using a LEO VP 1530 FEG SEM. XRD analysis was performed on the polished composite samples, the partially infiltrated foam and, for comparison, the un-infiltrated alumina foam. Small polished samples were used for the preparation of TEM samples in a Dual Beam Nanolab 600 FEI FIB. The samples were approximately 20 × 5 × 0.2 μm in size and produced across the alloy-Al_2O_3 interface. The foils were examined in a JEOL JEM 2000FX TEM and in a FEI F20 Tecnai field emission TEM/STEM system (EDS resolution 2 - 3 nm) for elemental analysis.

Results

Micrographs of the alumina foam and the infiltrated composite are shown in Fig. 1. From Fig. 1 (a), it can be seen that the foam had interconnected porosity in the form of approximately spherical cells connected by circular windows, a typical microstructure for the foams prepared using the gel-casting technique. Fig. 1 (b) and (c) show that the foam was completely infiltrated by the molten metal; the brighter phase is Al and the darker, Al_2O_3. The density measurements showed that the composites were between 98 - 99% of theoretical; the ~1% porosity being due to closed pores in the foam struts and / or metal shrinkage. From Fig. 1(c), good metal-ceramic bonding was seen and no bulk second phase was observed in the composite. Fracture surface observation of the composites after 3-point bending measurements showed good metal-ceramic interfacial bonding with cracks preferentially propagated through the ceramic phase. Data on the mechanical performance of the composites is being published elsewhere (Reference).

XRD scans of the infiltrated composite, Fig. 2, show that the composite consisted of α-Al_2O_3 and Al alloy. Due to the solid solution of Mg in Al, the Al peaks are slightly displaced, 0.3-0.8°, 2θ. The intensity of the Al_2O_3 peaks in the composite is comparatively much weaker than in the uninfiltrated ceramic foam. A strong peak representing the Al (111) plane, Fig. 2, was observed, which might indicate a preferred orientation in the composites.

Yellow-greenish compounds, believed to be Mg_3N_2 (Hou *et al.,* 1995), were observed on the partially infiltrated foams at the molten alloy-ceramic infiltration

front. XRD scans of this region support this view, Fig. 3, suggesting a chemical reaction between Mg and N_2 occurred during the infiltration process.

A typical TEM micrograph of the metal–ceramic interface is shown in Fig. 4 (a). No porosity was observed, which indicates good interfacial bonding. An EDS line-scan across the interface (Fig. 4 (b)) shows an increase in both Mg and N concentration; the line-scan position is shown in the micrograph. This interface layer could be categorized as one thin Al-O-Mg region near the ceramic and a continuous Al-N-O-Mg region near the Al. EDS line-scans across other infiltrated cells were performed and the same results obtained.

To further identify the interface compounds, diffraction patterns were taken. Fig. 5 shows an Al-Al_2O_3 interface, which was approximately 100 nm thick, together with a diffraction pattern from the Al-N-Mg-O layer (indicated by the arrow). Both AlN and Al_2O_3 were identified, although the latter might have been influenced by the Al_2O_3 foam. The AlN has a hexagonal structure and, from the figure, is fine grained and forms a continuous layer at the interface. The same analysis was performed on different TEM samples, another example is shown in Fig. 6, where AlN was again identified and observed to be continuous at the Al-Al_2O_3 interface. Although no AlN was detected by XRD, Fig. 2, this is probably a result of the small amount of the AlN formed at the metal-ceramic interface, making it difficult to detect by bulk XRD analysis. In contrast, when the composites were produced in a pure nitrogen atmosphere, AlN was detected by XRD due to the larger quantity formed [Binner *et al.,* in press].

$MgAl_2O_4$ was also detected at selective points in the Al-O-Mg region of the Al-Al_2O_3 interface. Fig. 7 (a) shows a spinel formed in this region with a face-centred cubic (FCC) structure. In addition, spinel was also observed inside of the Al_2O_3 foam strut; Fig. 7 (b) shows a spinel with a typical angular shape formed on the Al_2O_3 grain boundaries.

Fig. 8 shows another TEM micrograph of the alloy-ceramic interface in the composite. Interestingly, as well as the Al, Mg, O and N layer observed elsewhere, two Mg_2Si grains were also observed within the alloy matrix, close to the alloy-ceramic interface. This was the only example of Mg_2Si that was observed; the formation could be a result of a trace of Si being present in the master alloy, AZ81.

Discussion

It is well known that for pressureless infiltration, both Mg and N_2 are required; previous results showed that no infiltration occurred at the same temperature using an Ar atmosphere or without Mg in the alloy (Binner *et al.,* in press). In this research, Mg_3N_2 has been observed at the infiltration front (Fig. 3), whilst both Mg and N elements and a continuous AlN layer formed at the alloy-Al_2O_3 interface (Figs. 4 to 6). This demonstrates that chemical reactions, particularly, nitridation has happened in the system.

Based on the results, schematics of possible infiltration and interface development processes are presented in Fig. 9. At 915°C, the atmosphere between the molten Al(Mg) alloy and Al_2O_3 will have consisted of N_2 and evaporated Mg from the

molten Al alloy (Fig. 9 (a)). The Mg vapour can be expected to react with the N_2 to form Mg_3N_2 (reaction (1); $\Delta G_{915°C}$ = -213 kJ mol^{-1} (Hou *et al.,* 1995)), which may then deposit onto the surface of the Al_2O_3 foam. A possible interfacial morphology at this stage is shown in Fig. 9 (b). Mg_3N_2, however, when contacting molten Al, reacts with the Al to form AlN (reaction (2); $\Delta G_{915°C}$ = -175 kJ mol^{-1} (Hou *et al.,* 1995)). It is believed that it is this reaction that induces wetting and pressureless infiltration of molten Al into the ceramic foams (Schiroky *et al.,* 1997). At the same time, Mg is recycled in this reaction and it can dissolve into the molten metal and/or evaporate again.

The Mg vapour and/or the Mg_3N_2 may have reacted with the alumina foam to form Al-Mg-O spinel. In addition, Mg at the Al-Al_2O_3 interface of the infiltrated cells may diffuse along the Al_2O_3 grain boundaries towards the Al_2O_3 struts as well. One possible reaction is (Pai *et al.,* 1995):

$$3Mg + 4Al_2O_3 \rightarrow 3MgAl_2O_4 + 2Al$$

$\Delta G_{1000°C}$ = - 96.17 kJ mol^{-1} (Barin, 1989) (4)

where, in addition to spinel, Al is formed. A schematic of the interface microstructure, after AlN and spinel formation, is shown in Fig. 9 (c). To verify the presence of Mg in the foam, EDS maps of the Al_2O_3 strut in the composite were performed. The results (Fig. 10) show that Mg is present on the Al_2O_3 grain boundaries (Fig. 10 (b)), a result consistent with that in Fig. 7(b).

Hence, Mg_3N_2 is important in the aspect that it forms and disperses on the surfaces of the Al_2O_3 grains, which when contacting molten Al, reacts with the Al and drives the Al into the ceramic cells (pores). Besides the nitridation, diffusion of Mg at the alloy-ceramic interface and the localised formation of spinel may also be beneficial to infiltration in terms of reducing interfacial energy and improving wettability. It should also be noted that reaction of Mg with residual O_2, if there is any in the system, is important in gettering residual oxygen, preventing oxidation and facilitating nitridation (Sercombe & Schaffer, 2004). Finally, a continuous AlN interfacial layer has formed in the composite at the alloy-Al_2O_3 interface, which is important in obtaining good interfacial bonding and properties.

Conclusions

Al(Mg)/Al_2O_3 interpenetrating composites have been fabricated by pressureless infiltration in a N_2 atmosphere of Al-Mg alloy into gel-cast Al_2O_3 foams. Good metal-ceramic interface bonding has been observed in the composites. XRD analysis reveals that the composites contain only α-Al_2O_3 and Al, whilst Mg_3N_2 has been observed at the molten alloy-ceramic infiltration front. TEM analysis at the alloy-ceramic interface reveals that fine AlN, $MgAl_2O_4$ and Mg_2Si grains have formed. The results indicate that the infiltration is a capillary action, which is a result of improved wettability between the molten metal and the ceramic by complex chemical reactions.

Acknowledgement

The authors would like to thank EPSRC for the financial support and Dytech Corp. Ltd., UK, for supply of the ceramic foams. One of the authors (H. Chang) would like to thank the ORSAS Committee, UK, for financial support. Thanks are also extended to Mr. John Bates and Dr. Geoff West for their help in FIB and TEM operations.

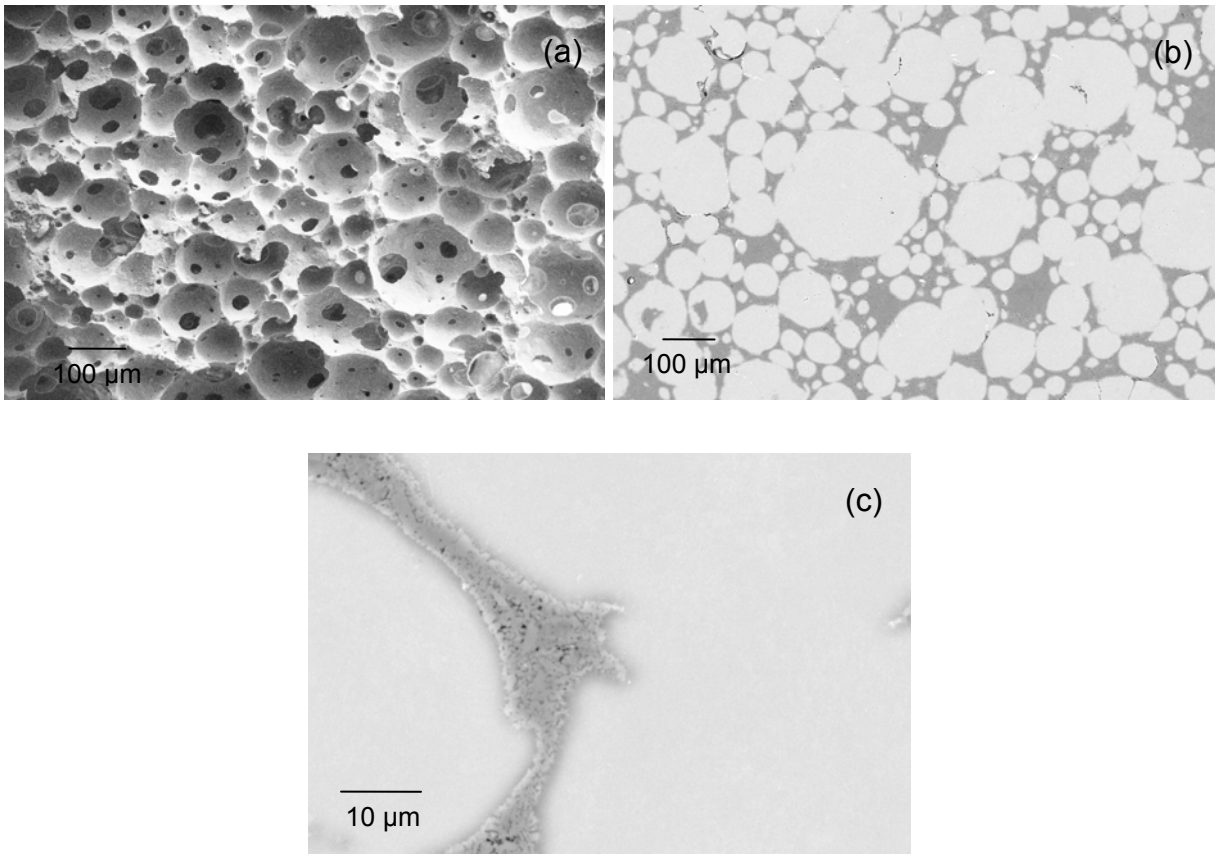

Fig. 1 SEM micrographs of (a) the original alumina foam and (b, c) the composites.

The composite images were taken using the back-scattered mode.

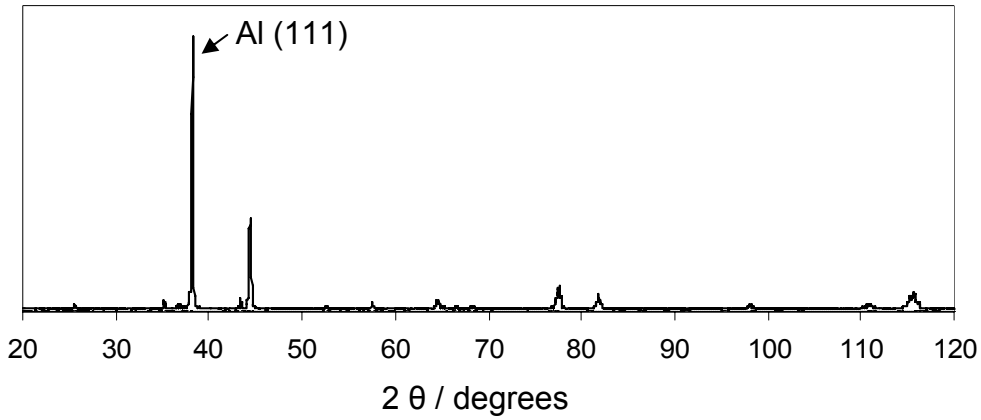

Fig. 2 XRD patterns of the Al-8Mg/Al_2O_3 composite.

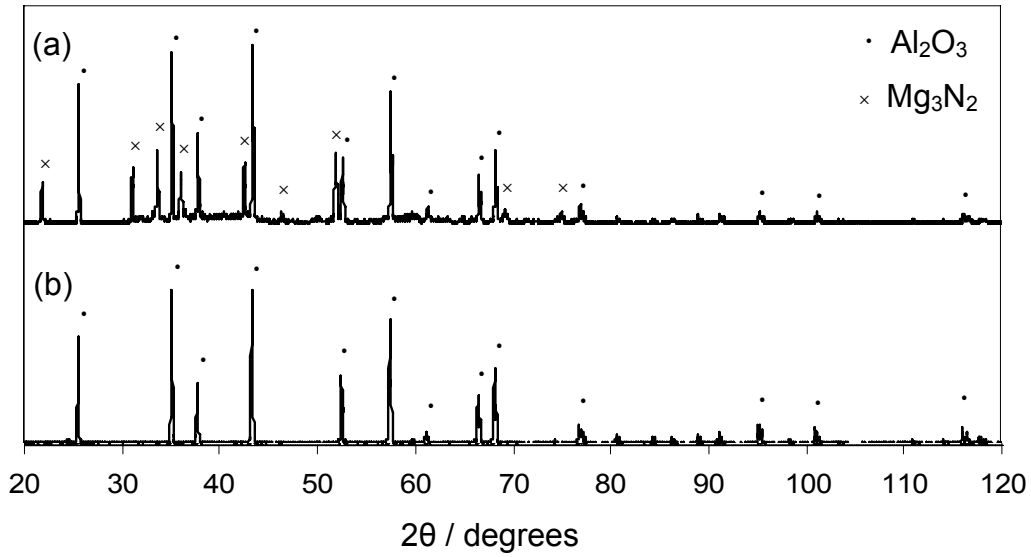

Fig. 3 X-ray analysis of (a) the alumina foam with the yellow-greenish compounds; (b) the original foam, for comparison.

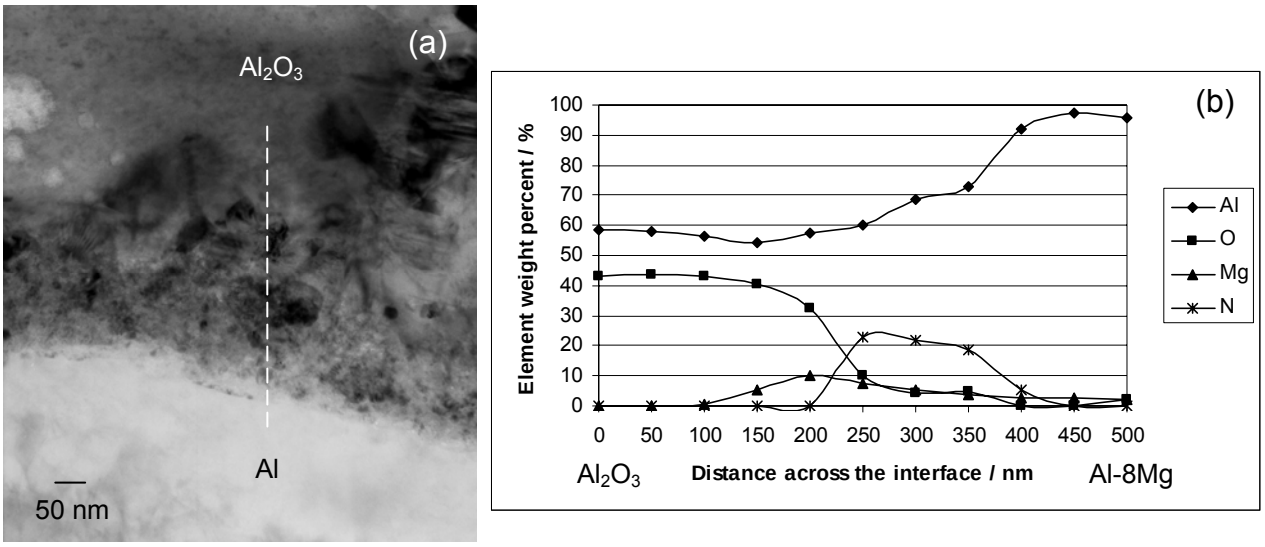

Fig. 4 Composite TEM micrograph at the metal-ceramic interface (a) and the TEM-EDS line analysis result across the interface (b).

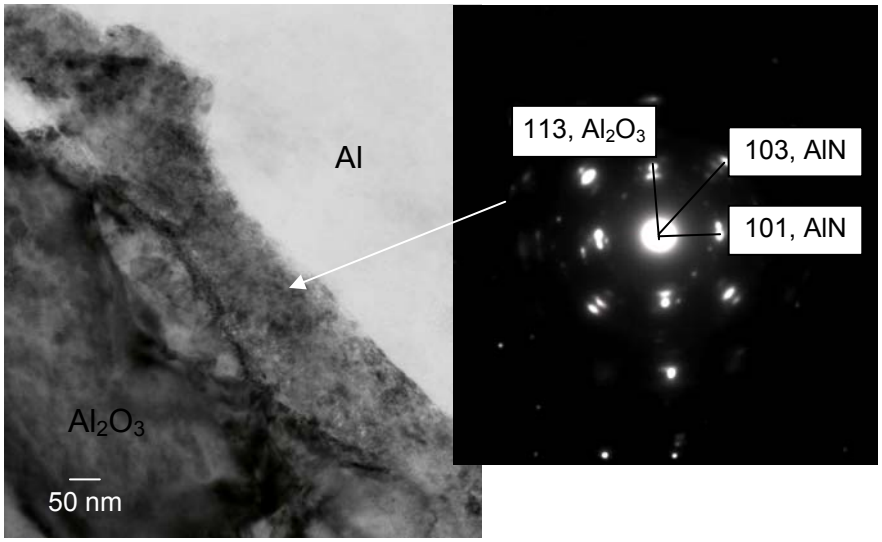

Fig. 5 TEM micrograph and the diffraction pattern of the AlN formed at the metal-ceramic interface in the composite.

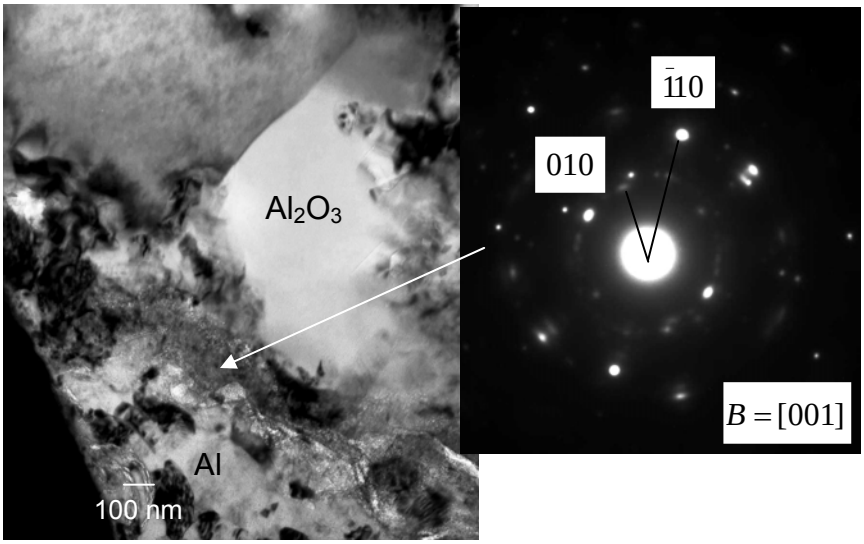

Fig. 6 TEM micrograph and the diffraction patterns of the AlN at the metal-ceramic interface in the composite.

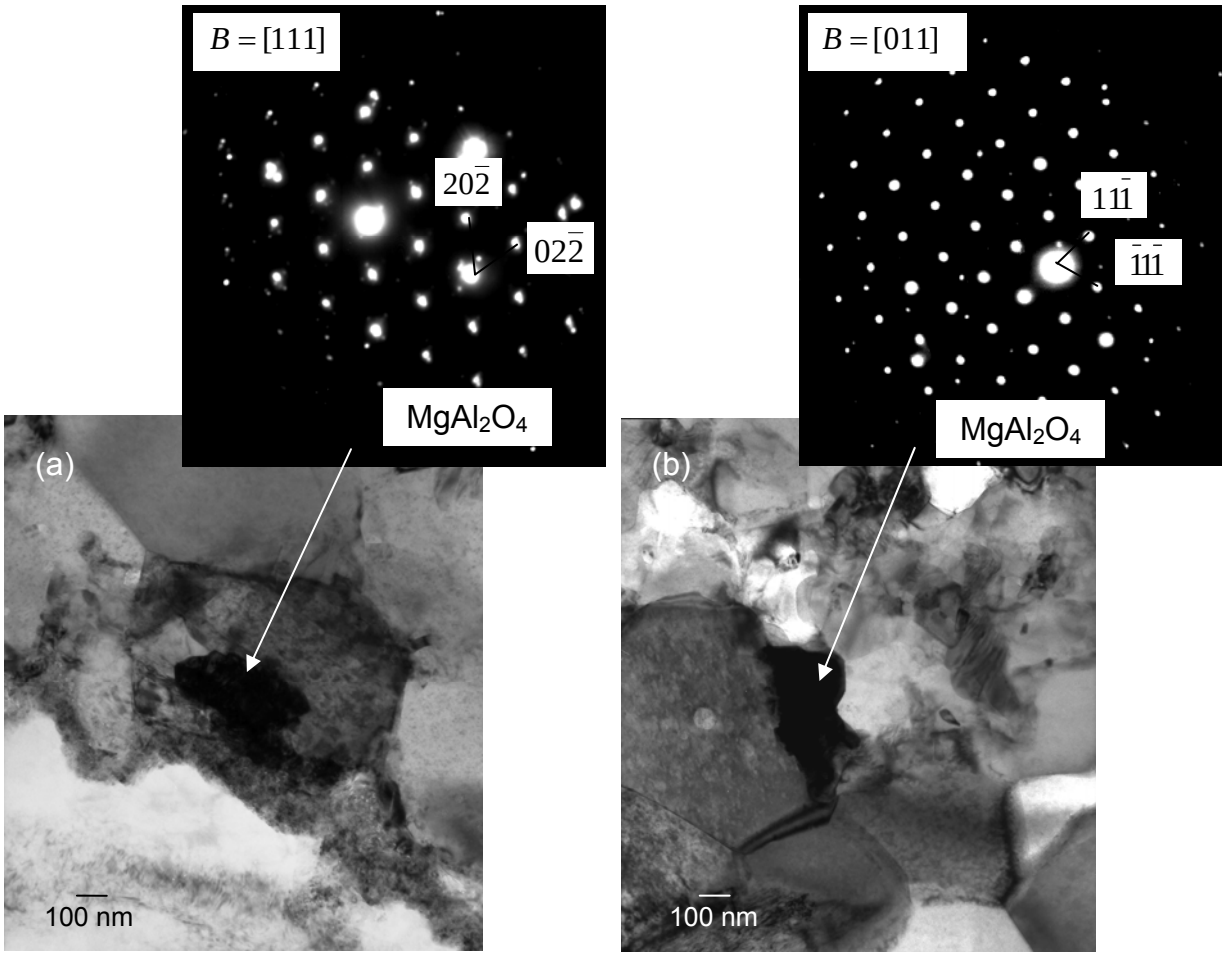

Fig. 7 TEM micrographs and diffraction patterns of the spinel formed (a) at the interface and (b) in the alumina foam strut within the metal-ceramic composites.

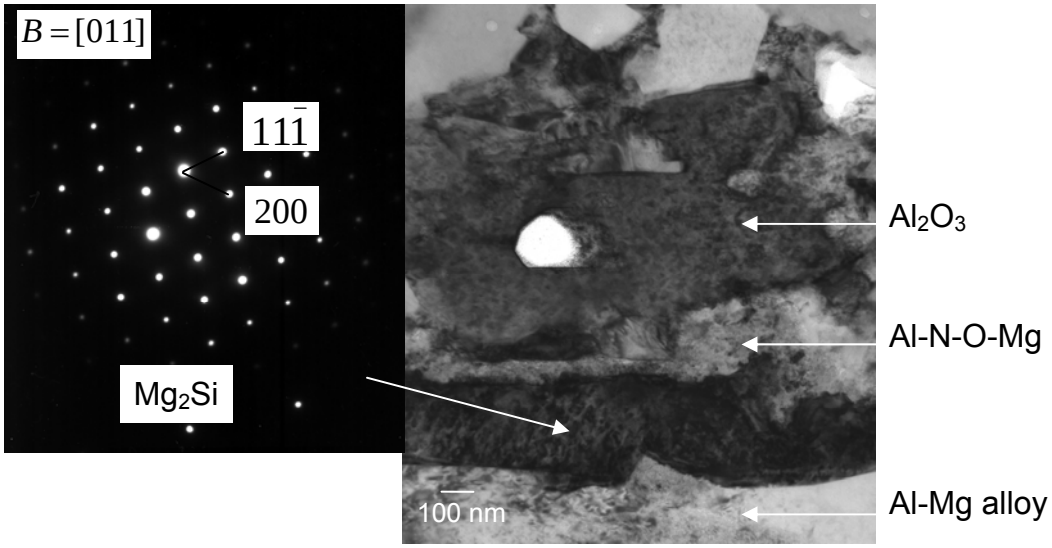

Fig. 8 TEM micrograph and the diffraction pattern of the Mg_2Si particle detected at the metal-ceramic interface.

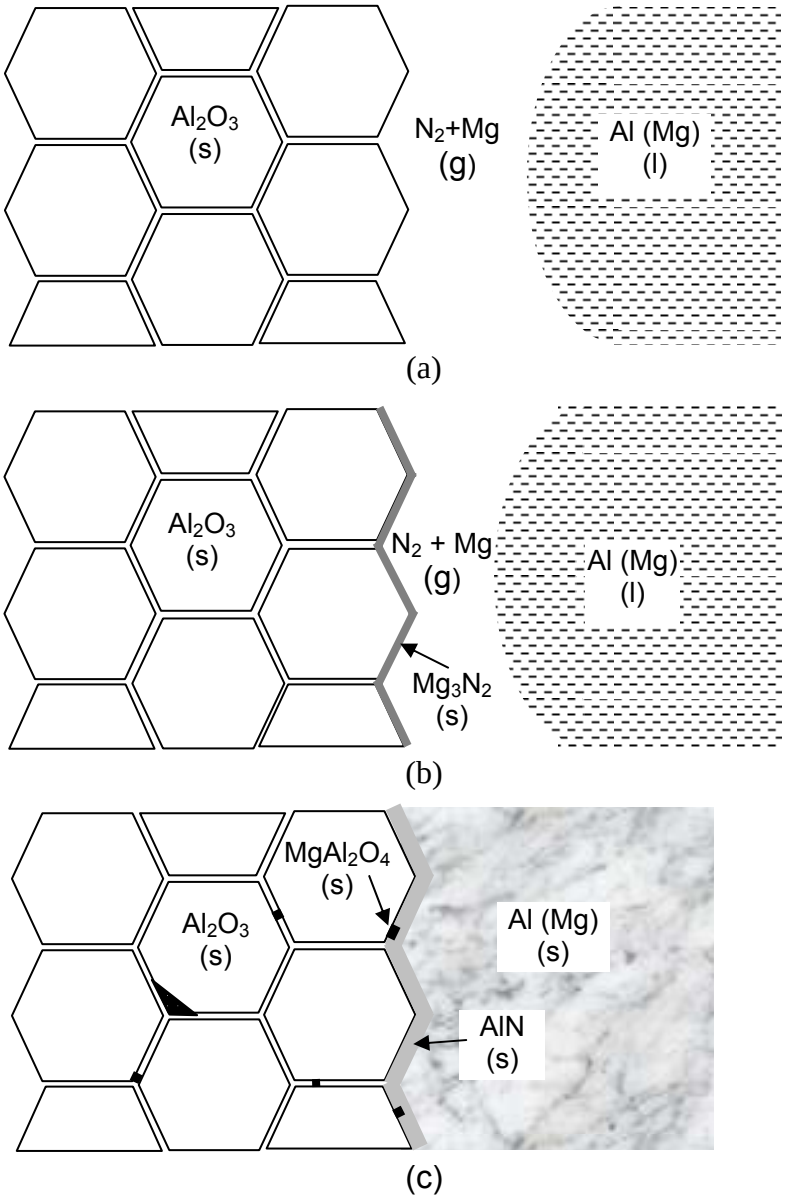

Fig. 9 Schematics of the reaction assisted infiltration and interfacial development processes: (a) at 915 °C, N_2 was introduced; (b) Mg_3N_2 formed and (c) metal-ceramic interface formed consisting of a continuous AlN layer and localized $MgAl_2O_4$.

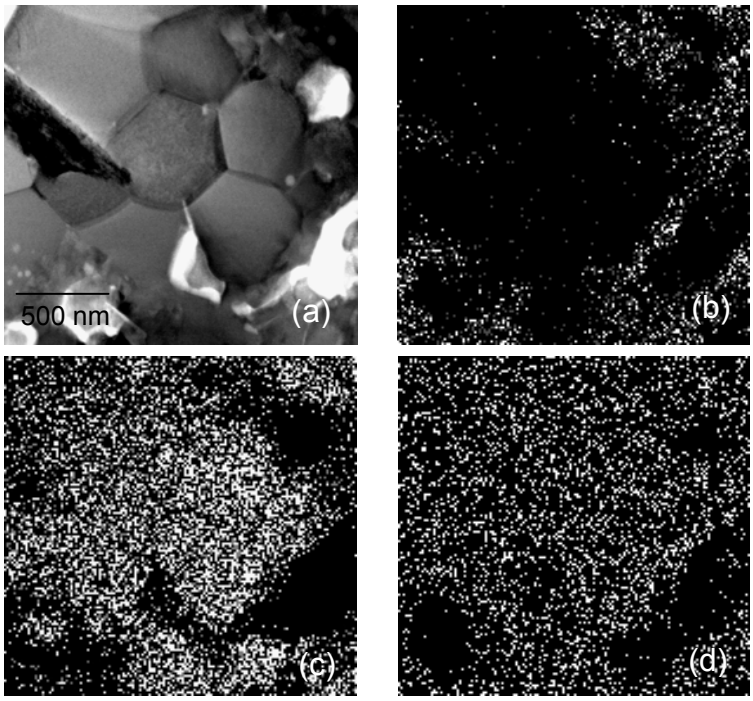

Fig. 10 TEM micrograph of (a) the alumina strut in the infiltrated composite, and the TEM-EDS maps: (b) Mg; (c) Al; (d) O.

References – shouldn't these be in alphabetical order?

Clarke, D. R. (1992) *Interpenetrating* Phase *Composites,* Journal of the American Ceramic Society, **75:** 4, 739-759.

Binner, J. G. P., Chang, H., Higginson, R. L. *Processing of Ceramic-Metal Interpenetrating Composites,* Journal of the European Ceramic Society, Special Issue, in press.

Aghjanian, M. K., Rocazella, M. A., Burke, J. T. *et al.* (1991) *The fabrication of metal matrix composites by a pressureless infiltration technique,* Journal of Material Science, **26**: 1, 447-454.

Zhong, L. J., Wu, J. B., Qin, J. T. *et al.* (1989) *An investigation on wetting behaviour and interfacial reactions of aluminium - α-alumina system,* in *Interfaces in metal- ceramics composites,* Lin, R Y and Arsenault, R J (Eds), *TMS,* Warrendale, PA, USA, 213-225.

Rao, B. S. and Jayaram, V. (2001) *Pressureless infiltration of Al–Mg based alloys into Al_2O_3 preforms: mechanisms and phenomenology*, Acta Materilia, **49**, 2373-2385.

Sercombe, T. B., Schaffer, G. B. (2004) *On the role of magnesium and nitrogen in the infiltration of aluminium by aluminium for rapid prototyping applications,* Acta Materilia, **52,** 3019–3025.

Saravanan, R. A., Molina, J. M., Narciso, J. *et al.* (2001) *Effect of nitrogen on the surface tension of pure aluminium at high temperatures*, Scripta mater, **44,** 965–970.

Lee, K. B., Kim, Y. S., Kwon, H. (1998) *Fabrication of Al-3 wt pct Mg matrix composites reinforced with Al_2O_3 and SiC particulates by the pressureless infiltration technique,* Metallurgical and Materials Transactions A, **29A,** 3087-3095.

Schiroky, G. H., Miller, D. V., Aghajanian, M. K. *et al.* (1997) *Fabrication of CMCs and MMCs using novel processes,* Key Engineering Materials, **127-131**, 141-152.

Hou, Q. H., Mutharasan, R., Koczak, M. (1995) *Feasibility of aluminium nitride formation in aluminum alloys*, Materials Science and Engineering A., **195,** 121-129.

Sepulveda, P., Binner, J. G. P. (1999) *Processing of cellular ceramics by foaming and in situ polymerization of organic monomers,* Journal of the European Ceramic Society, **19**: 12, 2059-2066.

Pai, B. C., Ramani, G., Pillai, R. M. *et al.* (1995) *Role of magnesium in cast aluminium alloy matrix composites*, Journal of Materials Science, **30,** 1903-1911.

Barin, I. (1989) *Thermochemical data of pure substances,* VCH Verlagsgesellschaft, Weinheim.